

See discussions, stats, and author profiles for this publication at: <https://www.researchgate.net/publication/257014670>

Damage mechanism and response of reinforced concrete containment structure under internal blast loading

Article in *Theoretical and Applied Fracture Mechanics* · October 2012

DOI: 10.1016/j.tafmec.2012.08.002

CITATIONS

12

READS

202

4 authors, including:



Chunfeng Zhao

Hefei University of Technology

19 PUBLICATIONS 69 CITATIONS

[SEE PROFILE](#)



Chen Jianyun

Dalian University of Technology

49 PUBLICATIONS 143 CITATIONS

[SEE PROFILE](#)



Damage mechanism and response of reinforced concrete containment structure under internal blast loading

C.F. Zhao^{*}, J.Y. Chen, Y. Wang, S.J. Lu

Institute of Earthquake Engineering, Dalian University of Technology, Dalian, 116024 Liaoning, China

ARTICLE INFO

Article history:
Available online 31 August 2012

Keywords:
Damage mechanism
Reinforced concrete containment
Numerical simulation
Blast loading
Scale distance
ALE

ABSTRACT

Reinforced concrete containment (RC) is the most significant component of the nuclear power plant. It may lead to serious disaster owing to the leakage of radioactive materials as the reasons of internal explosion of reinforced concrete containment caused by earthquakes, fires, gas explosions or terrorist attacks, etc.

The objective of this paper is to investigate the behavior of reinforced concrete containment, numerical simulation taking into account fluid–solid coupling interaction is conducted for the analysis on the dynamic responses of reinforced concrete containment under internal blast loading using LS–DYNA software, especially focusing on its damage mechanism.

The generation and the propagation of blast wave and its effect on a containment structure are discussed using Arbitrary Lagrangian Eulerian (ALE) algorithm and multiple material models. The analysis results of the containment have been compared by empirical equations. Parametric studies have also been performed for internal detonation under different scale distances at a standoff distance of 20 m in the RC containment. The results indicate that the influences of scale distances and mesh qualities of structure on dynamic response and damage mechanism of the structure are analyzed to assess the structural anti-explosion capability.

© 2012 Elsevier Ltd. All rights reserved.

1. Introduction

Reinforced concrete containment of nuclear power plant must be constructed and operated in order to protect the population and environment against an uncontrolled release of radioactivity in the event of severe internal or external accident occurrence, such as large fires, earthquakes, jet aircraft impact, that might be expected during the plant lifetime [1]. Studies are reported in literature [1–5] on the impact of an aircraft on the outer reinforced concrete nuclear containment shells, but the scarce on the effect of explosions in the reinforced concrete containment shells until Fukushima nuclear event March 2011.

Many works have been done to calculate the dynamic plastic responses of reinforced concrete structures when subjected to explosion loading. Dong et al. studied the strain growth in containment vessels caused by non-linear modal coupling in the non-axisymmetric response of complete spherical containment vessels subjected to internal blast loading [6]. Lin et al. studied the thermal decomposition and thermal explosion hazard for HNIW and HMX to predict the best storage conditions that allow avoiding any violent runaway reaction [7]. The dynamic plastic responses of discrete multi-layered explosion containment vessels with considering the

effects of strain-hardening and strain-rate were analyzed by Chen et al. [8].

So far, in work [9], non-linear response of reinforced concrete containment structure under blast loading has been studied by Pandey et al. using appropriate non-linear material models till the ultimate stages to demonstrate the effect of an external explosion on the outer reinforced concrete shell of a typical nuclear containment structure. Hu and Lin used the ABAQUS finite element program to predict the ultimate pressure capacity and the failure mode of PWR prestressed concrete containment at Maanshan nuclear power plant [10]. Keivan et al. investigated the response of reinforced concrete structure due to axisymmetric macrocell corrosion of rebar is of concern after propagation of microcracks within the concrete medium [11]. Bao and Li utilized a high-fidelity physics-based computer program, LS–DYNA to provide numerical simulations of the dynamic responses and residual axial strength of reinforced concrete columns subjected to short standoff blast conditions, then discussed the finite element model and verified through correlated experimental studies [12]. Hao et al. conducted numerical analysis on the elastic–plastic dynamic response of steel columns subjected to pressure wave from an underground explosion [13]. Sheng et al. performed an analysis on explosive damage to reinforced concrete columns [14]. In respect to the explosion resistance of walls, Nash et al. examined the spall damage to concrete walls from close-up cased and uncased explosions in the air

^{*} Corresponding author.

E-mail address: zhaowindy@126.com (C.F. Zhao).

[15]. Varma et al. discussed the damage to brick masonry panel walls under high explosive detonations [16]. Makovicka studied the dynamic response of thin masonry walls under explosion effects [17]. Mays et al. considered the dynamic response to the blast load of concrete wall panels with openings [18]. Therefore, an analytical model with considering the effect of strain rate should be conducted with fluid-structural algorithm in order to have a better understanding on the dynamic response of RC containment.

The present study has therefore been directed to study the effect on internal explosions on a typical reinforced concrete containment structure. Prediction of response of concrete structures for blast loading requires three-dimensional structural idealizations, true modeling of the material non-linear and precise modeling of the blast phenomenon. Different aspects of non-linearity in concrete, such as pressure sensitivity in three-dimensional loading situations, mesh quality sensitivity in dynamic loading situations and failure of concrete in tension have been included in developing finite element software and different parametric analysis has been performed.

Numerical simulation of the blast loading parameters for a specified scale distance for reinforced concrete containment is very significant in precise determination of the response. Most parameters for modeling the blast shock waves interactions as available for different parameters have been expressively stated. The dynamic response and damage mechanism of the reinforced concrete containment are investigated subjected to internal blast loading at varying scale distances. The effect of explosion inside of containment has been presented in terms of the extent of cracking in the concrete, stress in steel bar and concrete after yielding and deflections.

2. Fundamental theories

2.1. Description of last load parameters

The sudden release of energy from an explosive in the air produces an instantaneous high temperature, high pressure detonation wave in the atmosphere. The pressure wave causes a rapid expansion and propagation of ambient gases, and the high pressure air at the front end of these gases contains most of the explosive energy is known as the blast pressure wave. The energy carried by the blast pressure wave will decrease as the propagation distance and time increase and the pressure behind the shock wave front can instantly reduce to below the air pressure of the surrounding atmosphere. During the negative pressure phase, the air evacuated to create a vacuum and the pressure and temperature then return to the same as the ambient air. The variation of the over pressure with time for a typical shock at a particular location is shown in Fig. 1. Before the arrival of the shock wave, the atmosphere pressure is P_a at t_a . The pressure suddenly rises to maximum over pressure peak P_{so} after the explosion, then decays to

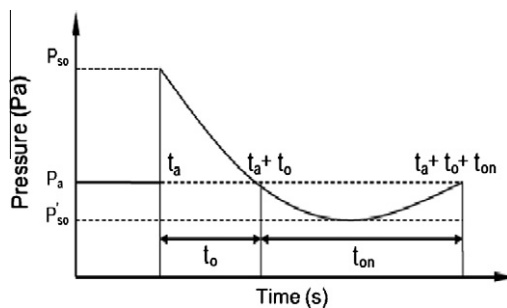


Fig. 1. Variation of blast pressure with time at a specified distance.

P_a at $t_a + t_o$, later falls below the atmospheric pressure to the negative pressure peak P'_{so} , and finally returning to P_a at $t_a + t_o + t_{on}$ [19].

It is difficult to obtain the parameters of the blast pressure wave through theoretical analysis due to the complexity of the explosion process. Baker proposed an equation to express the pressure attenuation process [20]:

$$P_{so}(t) = P_{so} \left(1 - \frac{t}{t_o} \right)^{-t/e^{t_o}} \quad (1)$$

Here, t is duration time of the pressure wave travel from the explosion to the given location. The impulse formed by positive pressure can be obtained using its integral to time.

$$i_{so} = \int_{t_a}^{t_a+t_o} P_{so}(t) dt \quad (2)$$

Some studies have proposed some usable empirical equations for shock wave parameter calculation through theoretical analysis and numerical simulations. The commonly used empirical equations include that proposed by [21]:

$$\left. \begin{aligned} P_{so} &= 1.4072Z^{-1} + 0.554Z^{-2} - 0.0357Z^{-3} + 0.000625Z^{-4} (0.1 \leq Z \leq 0.3) \\ P_{so} &= 0.619Z^{-1} - 0.033Z^{-2} + 0.213Z^{-3} (0.3 \leq Z \leq 1) \\ P_{so} &= 0.066Z^{-1} - 0.405Z^{-2} + 0.329Z^{-3} (1 \leq Z \leq 10) \end{aligned} \right\} \quad (3)$$

Consider [20]:

$$\left. \begin{aligned} P_{so} &= 20.06Z^{-1} + 1.94Z^{-2} - 0.04Z^{-3} (0.05 \leq Z \leq 0.5) \\ P_{so} &= 0.67Z^{-1} + 3.01Z^{-2} + 4.31Z^{-3} (0.5 \leq Z \leq 70.9) \end{aligned} \right\} \quad (4)$$

And Brode's equation [22]:

$$\left. \begin{aligned} P_{so} &= \frac{0.975}{Z} + \frac{1.455}{Z^2} + \frac{5.85}{Z^3} - 0.019 \quad 0.1 < P < 10 \text{ bar} \\ P_{so} &= \frac{6.7}{Z} + 1 \quad P_{so} > 10 \text{ bar} \end{aligned} \right\} \quad (5)$$

where Z is the scaled distance, expressed by $Z = R/W^{1/3}$, R is the standoff distance and W is the mass of explosive.

2.2. Blast wave scaling laws

The most widely used approach to blast wave scaling is the cube root scaling law proposed independently by Hopkinson [23] and Cranz [24]. The law states that, similar blast waves are produced at identical scaled distances when two explosive charges of similar geometry and of same explosive but of different sizes are detonated in the same atmosphere. Thus if charges of weights W_1 and W_2 are detonated then the same peak pressure is produced at distance of R_1 and R_2 , respectively. The distances R_1 and R_2 are related as given below [9]:

$$\frac{R_1}{R_2} = \left(\frac{W_1}{W_2} \right)^{1/3} \quad (6)$$

The duration of positive phase of a pressure wave is also given by a similar equation.

3. Analysis of reinforced concrete containment subjected to blast pressure wave

3.1. Arbitrary-Lagrangian-Eulerian (ALE) algorithm

In general, there are two classical algorithms often used with finite meshes for continuum such as Lagrangian and Eulerian algorithm. In the Lagrangian algorithm, nodes on meshes can be moved with material points, and element meshes can be deformed. In the Eulerian algorithm, element meshes are fixed in space, and

the material points move in pre-planned meshes. Element meshes do not deform during the movement of an object, so that large fluid meshes are to be planned appropriately.

In the analysis model built upon Lagrangian elements for explosives and ambient mediums, the finite element mesh instantly distorts when studying the blast pressure wave effects on the structure and the medium moving with the explosives. Hence, the Jacobian of the integration point may become a negative value and the stable time step size needed for the calculation approaches zero. As a result, either the overall computing time extends infinitely or the computing process diverges. If the model is built using Eulerian elements and the mesh remains unmoved, numerous Eulerian elements are required to trace the dynamic response of the structures, which may cause errors due to the computation of complex changes to the interface. Therefore, this study applied the ALE method, which integrates the advantages of the Lagrangian and Eulerian elements but without the excessive mesh distortion problem, to the proposed method effectively, traces the movement of structural boundaries and observes the blast pressure wave's pressure distribution in the medium while the blast load is occurring [11].

3.2. Constitutive laws and equation of state (EOS)

In the finite element model of a continuum, the RC containment model was discretized into finite number of sections over which the conservation and constitutive equations are solved. There are four materials in this study such as explosive, air, steel and concrete. An appropriate constitutive material model and equation of state for each material need to be considered. Hence, the ALE models of the explosion are applied to calculate the pressure throughout the mesh. The ALE model is computationally more expensive than the Lagrangian model, and is only appropriate for small standoff distances. The material parameters and constitutive models employed in this paper were shown in Table 1 and describe below [25].

3.2.1. Explosive

For explosive material, *MAT_HIGH_EXPLOSIVE_BURN is used. The JWL equation of state is necessary to simulate the behavior of an explosive, its detonation velocity is 6930 m/s, and EOS is expressed as follows:

$$P = A \left(1 - \frac{\omega}{R_1 V} \right) e^{-R_1 V} + B \left(1 - \frac{\omega}{R_2 V} \right) e^{-R_2 V} + \frac{\omega E}{V} \tag{7}$$

where A, B are linear explosion parameters; ω, R_1 and R_2 are non-linear explosion parameters; V is relative volume and E is specific internal energy of every unit of mass. The JWL EOS is used for determining the pressure of the detonation products of high explosives. According to the explosives manual [26], JWL EOS parameters of TNT are shown in Table 1.

3.2.2. Air

The linear-polynomial EOS is used to model the behavior of the air and linear in internal energy. The pressure is given by:

$$P = C_0 + C_1 \mu + C_2 \mu^2 + C_3 \mu^3 + (C_4 + C_5 \mu + C_6 \mu^2) E_0 \tag{8}$$

where E_0 is the specific initial energy, and $\mu = \rho/\rho_0 - 1$, C_i ($i = 0-6$) are the coefficients. For the ideal gases, the coefficients in the EOS are setting as $C_0 = C_1 = C_2 = C_3 = C_6 = 0$, and $C_4 = C_5 = \gamma - 1$, γ is the polytropic ratio of specific heats. The pressure is then given by:

$$P = (\gamma - 1) \frac{\rho}{\rho_0} E_0 \tag{9}$$

where ρ/ρ_0 the ratio of current density to reference density, γ is the ratio of specific heats, ρ_0 is the initial density of air, and ρ is the current density of air. E_0 is the specific initial energy, with the gamma law EOS under standard atmospheric pressure and $\gamma = 1.4$, its initial energy is $E_0 = 2.5 \times 10^5$ J/kg.

3.2.3. Steel bar

A plastic kinematic model with a hardening effect is applied for simulate steel bar. The elastic-plastic behavior of the material with kinematic and isotropic hardening is shown in Fig. 2, in which l_0 and l are the undeformed and deformed lengths of uniaxial tension specimen. E_t is the plastic slope of the bilinear stress strain curve. $\beta_0 = 0$ is for kinematic hardening and $\beta_0 = 1$ is for isotropic hardening. The present study assumes $\beta_0 = 0$ [27].

3.2.4. Concrete

For purposes of simplicity and cost efficiency, concrete is assumed to undergo elastic deformation and isotropic elastic plastic model is applied in this paper.

Table 1
The material parameters of the reinforced concrete containment for internal explosion analysis.

Material	(unit = cm, g, μ s, Mbar)						
Air	*MAT_NULL						
	Mass density (g/cm ³)						
	0.00125						
Explosive	*EOS_LINEAR_POLYNOMIAL						
	C_0	C_1	C_2	C_3	C_4	C_5	C_6
	0	0	0	0	0.4	0.4	0
	*MAT_HIGH_EXPLOSIVE_BURN						
	Mass density (g/cm ³)	Detonation velocity (cm/ μ s)	C–J pressure (Mba)				
	1.63	0.693	0.27				
	EOS_JWL						
	A (Mba)	B (Mba)	R_1	R_2	ω	E (Mba)	V
3.71	0.0743	4.15	0.95	0.3	0.07	1	
Steel bar	*MAT_PLASTIC_KINEMATIC						
	Mass density (g/cm ³)	Young's modulus (Mba)	Poisson's ratio	Yield stress (Mba)	Tangent modulus (Mba)		
	7.8	2.1	0.3	0.00414	0.0013		
Concrete	*MAT_ISOTROPIC_ELASTIC_PLASTIC						
	Mass density (g/cm ³)	Shear modulus (Mba)	Yield stress (Mba)	Tangent modulus (Mba)	Bulk modulus (Mba)		
	2.65	0.10868	0.025	0.021	0.02746		

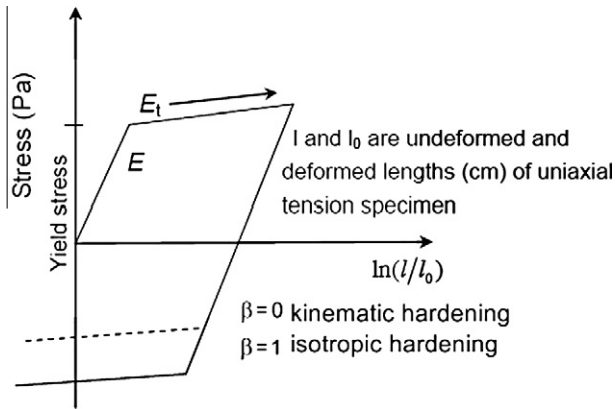


Fig. 2. Plastic kinematic model.

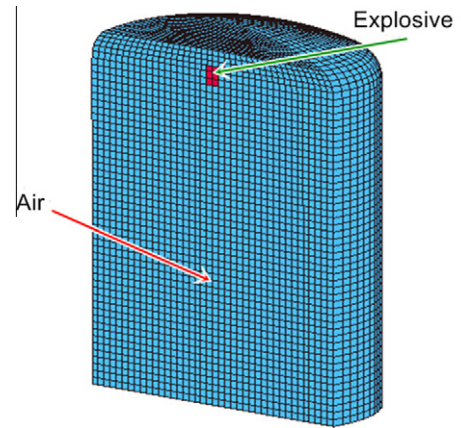


Fig. 5. The Eulerian meshes.

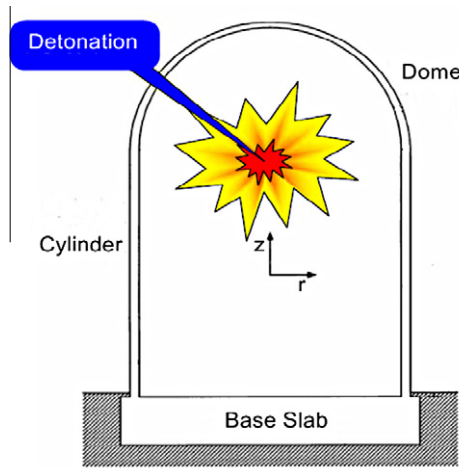


Fig. 3. The internal explosion diagram of reinforced concrete containment.



Fig. 6. The Lagrangian meshes.

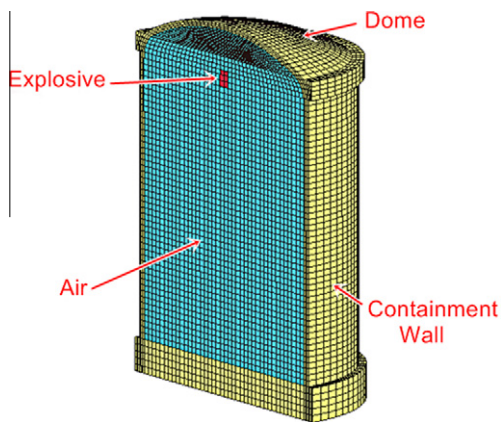


Fig. 4. Finite element model.

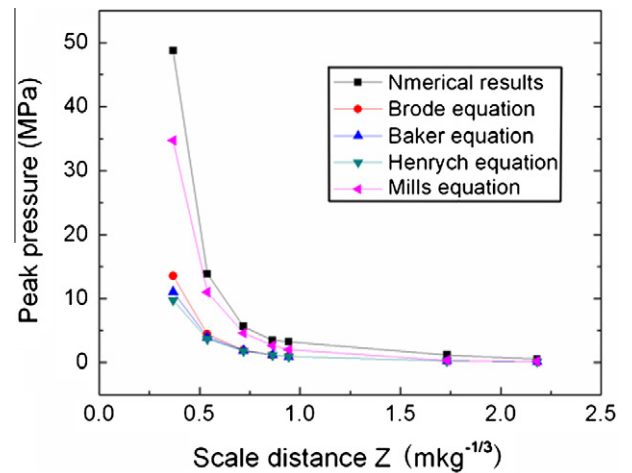


Fig. 7. Variation of peak pressure with scale distance in the numerical simulation and empirical equation.

4. Description of analysis model

The reinforced concrete containment is composed of a circular base slab, an upright cylinder and a hemispherical dome. To simplify the analysis, the tendon gallery, equipment hatches and penetrations on the containment are not considered and the structural geometry is assumed to be axisymmetric. The base slab of the

containment is embedded in the soil and the basic geometry of the simulation is shown in Fig. 3.

The cylindrical part has an inner diameter of 40.0 m, outer diameter is 42.2 m and the height of 48.0 m; the hemispherical

dome has an inner diameter of 20.0 m, outer diameter of 20.9 m and the thickness of 0.9 m; the total height of reinforced concrete

containment is 68.9 m. Two buttresses are installed at the horizontal angles of 0 and 180 and the volume is more than 60000 m³. The

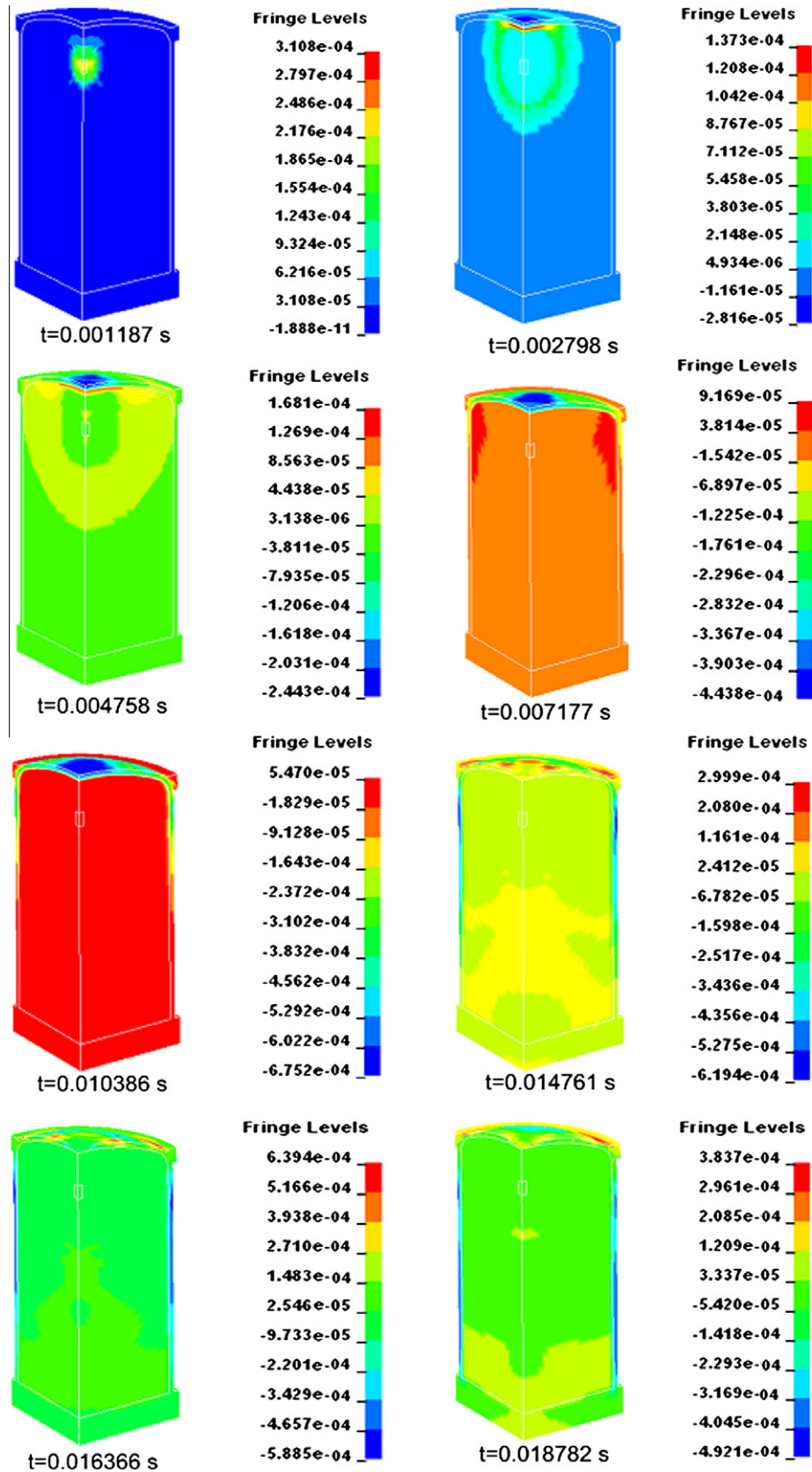


Fig. 8. Fluid-structure-interaction for explosion process at scale distance of $0.778 \text{ m/kg}^{1/3}$ for a distance of 20 m.

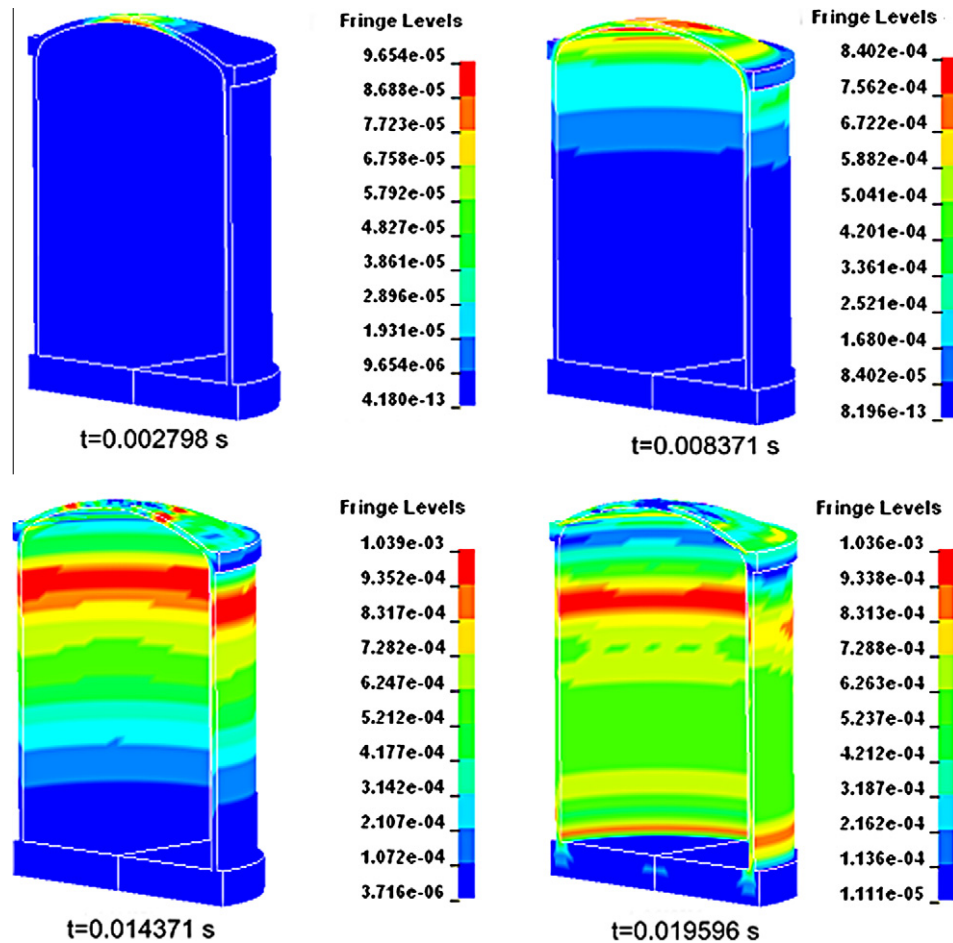


Fig. 9. Von mises stress of the RC containment at scale distance of $0.778 \text{ m/kg}^{1/3}$ for a distance of 20 m.

explosives were located in the center of the containment shell and 48.0 m above the containment base slab. The structure and load were symmetrical, so one fourth the model was taken for analysis in order to simplify the computing. For simplicity, the lateral pressure applied to the base slab due to soil is not considered [11].

The finite element model of the structure is shown in Fig. 4. During the computing process, the explicit time integration method was employed to compute the time integration. Since it is a conditional stable integration method and the integration time step size is function of the characteristic mesh length. If the mesh length was very small and thus the computation time would increase sharply.

4.1. numerical model of fluid–structure–interaction

In this fluid–structure interaction model, both the explosive and air are modeled with Eulerian meshes, while the steel bar and concrete are modeled with Lagrangian meshes. For obtaining accurate solutions, one Lagrangian element must cover two Eulerian elements when coupling the two meshes.

As the Lagrangian and Eulerian algorithms taken to establish various simulation models, the air and explosive are mixed during the shock wave propagation process. Therefore, air and explosives models can be regarded as fluid, established by Eulerian meshes and computed with multi-material ALE algorithm shown in Fig. 5. The containment shell is regarded as solid, established by Lagrangian meshes shown in Fig. 6.

4.2. Bonding relationship between reinforced steel and concrete

Generally, in the non-linear finite element analysis of reinforced concrete containment, reinforced effect simulation utilizes three methods: separation model, smeared mode and entirety mode. If the local damage of the reinforced concrete is subjected to an explosion effect, the separate type should be adopted as the composite mode and the entirety mode have a poor computing accuracy and cannot observe the damage of reinforced steel. Therefore, separate type model is adopted for analysis in this study. Reinforced steel is performed with the beam element and hexahedron continuum elements are used for simulation concrete. The CONSTRAINED-LAGRANGE-IN-SOLID command is used to define the bonding of reinforced steel and concrete coupled the reinforced steel element and concrete element. It was supposed that there was a high bond between the concrete and reinforced steel subjected the instantaneous internal impulse force effect without sliding between them.

5. Results and discussion

In order to validate the accuracy of the analysis results, a free field explosion simulation was conducted and the blast pressure wave parameters were compared in this paper. Fig. 7 shows a comparison of the numerical simulation and the peak pressure results according to the different empirical equations such as Baker,

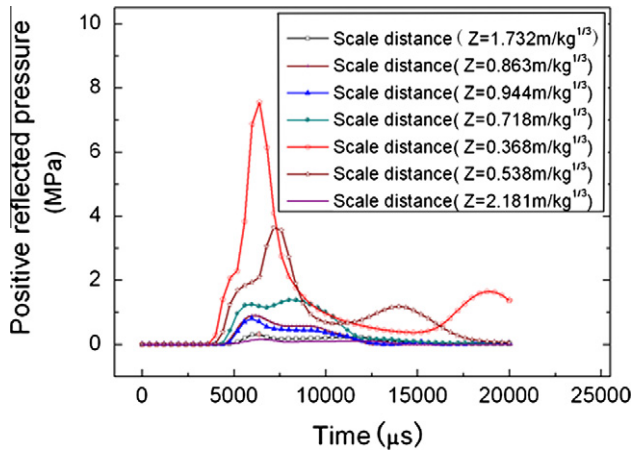


Fig. 10. Variation of positive reflected pressure with time for internal blast of different scale distance at a detonation of 20 m.

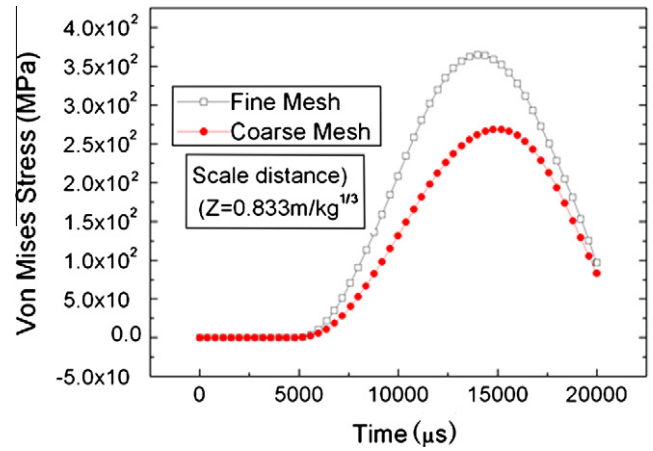


Fig. 12. Von mises stress of reinforcing bar versus time curve for fine mesh and coarse mesh at top of containment.

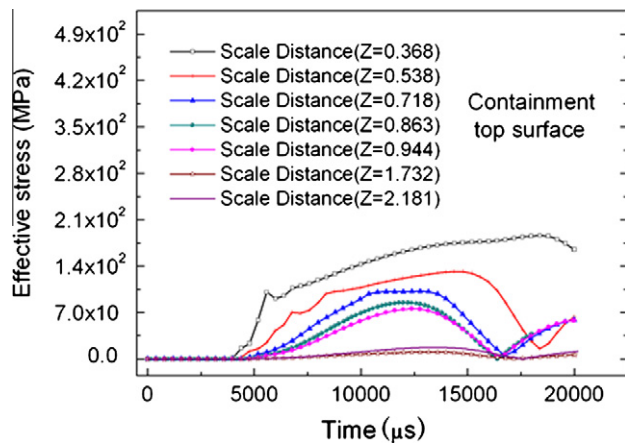


Fig. 11. Variation of effective stress with time for internal blast of different scale distance at a detonation distance of 20 m on top surface of containment.

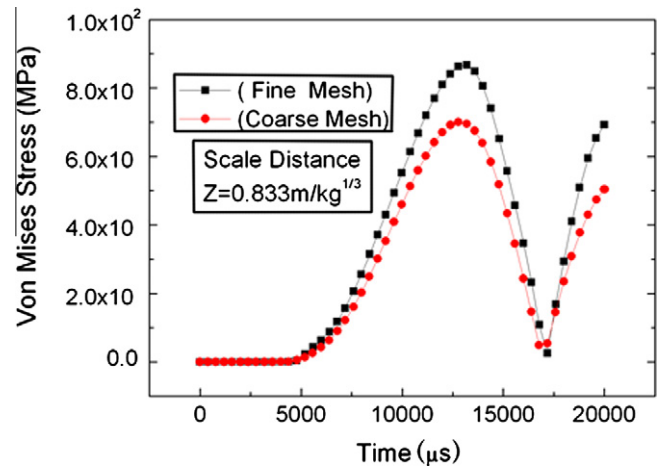


Fig. 13. Pressure of containment shell with time history for different mesh quality at $Z = 0.833 \text{ m/kg}^{1/3}$.

henrych, Brode, and mills equation under different scale distance Z , ($Z = R/W^{1/3}$, W is explosive charge) [20–22].

As shown in the Fig. 7, the peak pressure wave curve, as simulated by this study, indicates the same trend as the empirical equation results. However, the numerical result 48.76 MPa is for $Z = 0.368 \text{ m/kg}^{1/3}$. The peak pressure is calculated according to Eq. (3) is 9.76 MPa, Eq. (4) is 11.05 MPa, and Eq. (5) is 13.07 MPa for $Z = 0.368 \text{ m/kg}^{1/3}$. It is noted that peak pressure of the numerical results for $Z = 0.368 \text{ m/kg}^{1/3}$ is much larger than empirical equation results and the trend is consistent with the empirical equation results when scale distance greater than $1 \text{ m/kg}^{1/3}$, which indicates that the action of the reflected wave in airtight container has great influence on the pressure–time history curve.

5.1. The fluid field and interaction between the pressure wave and containment

The computed load distribution of the near field due to the explosion inside of the RC containment is shown in Fig. 8. The propagation of the shock wave in the structure and above 48 m of the base at different time instants is clear observed. It is also found that the blast shock wave arrived to the dome at first when the explosive denoted due to the standoff distance between the explosion source and the dome is the nearest of all the distances. In the process of the

pressure wave propagation, the reflected pressure wave will be produced when the positive pressure wave action on the containment and then the pressure intensity of shock wave enhanced as the interaction of reflected wave and shock wave.

Fig. 9 shows the contours of the effective stress of the containment dome and wall. It can be seen from the Fig. 9 that the top of dome may be the weakest position in the containment due to the strong pressure wave firstly arrived and impact on it. Therefore, the dome of the containment may be the first failure when the gas explosion in the containment, just as Fukushima nuclear event at March 11, 2011. Therefore, RC containment dome should be strengthened when design and construct the nuclear power plant.

5.2. The effect of scale distance on the structure

The positive reflected pressure and the containment inner surface stress scale distance history analysis results are displayed in Fig. 10. As shown in Fig. 11, the positive reflected pressure at the top of containment wall for various scale distance reaches the maximum value within a very short time and then instantly decreases to ambient pressure. It is also observed that the positive pressure decrease with the scale distance increasing due to the small scale distance at the same distance from explosive source has larger quantity explosive charge induce shock wave with high

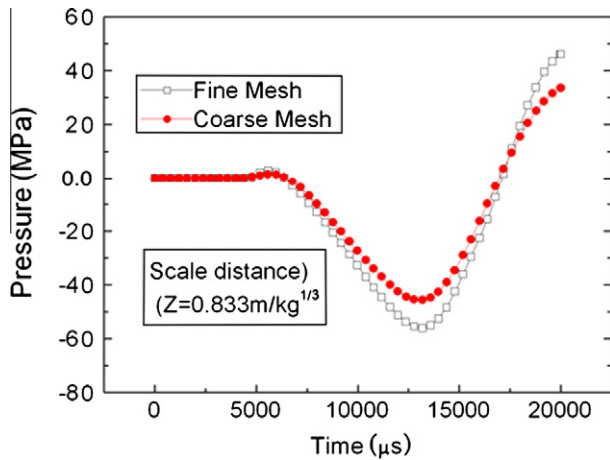


Fig. 14. Von mises stress with time history curve at top of containment dome for different mesh quality at $Z = 0.833 \text{ m/kg}^{1/3}$.

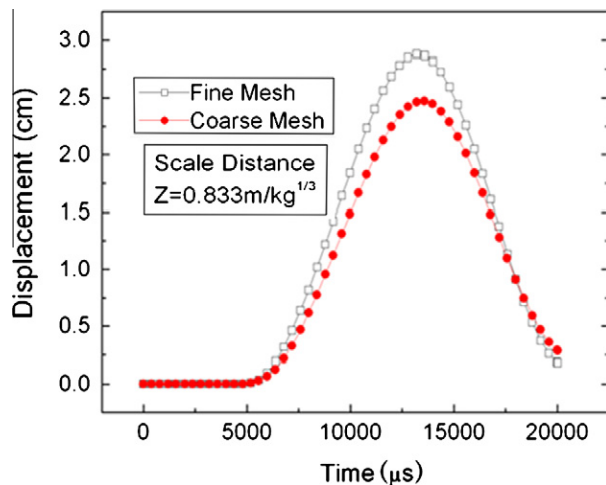


Fig. 15. Displacements with time history at top of containment dome for different mesh quality at $Z = 0.833 \text{ m/kg}^{1/3}$.

energy. The top point of the containment is significantly affected by the explosion; the pressure of concrete for containment top surface is much more than the design internal pressure 0.4 MPa as shown in Fig. 11. Therefore, the containment has insufficient resistance that it cannot bear a largest portion of the blast load at these scale distance.

As above discussed, the scale distance has a more significant effect on the response of containment. This is because, with the increasing of scale distance, the explosive charge and the values of overpressure will decrease. This will generate blast wave with little energy, leading to the small dynamic response on the containment.

5.3. The effect of elements qualities

In order to validate the accuracy of the analysis results, the element size effect of RC containment is also investigated in this section. For comparison purposes of simplicity, two element sizes are considered.

Fig. 12 displays the stress time history and the variation of reinforcing bar's axial stress history analysis results. It can be seen from the Fig. 12 that the horizontal axial stress at the profile of steel bar is 365 MPa at $Z = 0.833 \text{ m/kg}^{1/3}$, which is small than the yield stress of steel bar 414 MPa. The von mises stress and attenuation differ due

to the different mesh sizes, the period of stress vibration and amplitude increases with the decrease in the dimensional size of element for reinforcing bar, i.e. the better element quality, the more accurate results. This indicates that the mesh quality has great influence on the stress history curve of steel bar.

Figs. 13–15 show a time history comparison of the finite element mesh to the pressure on the concrete surface. It is observed that the concrete of the containment has a similar effect of reinforcing bar at the same scale distance, i.e. the pressure, displacement and stress of concrete increase with mesh size decreases. In other word, if the element has a better mesh quality, the numerical results of the structure are slightly larger than that of with bad mesh quality which more closer to the actual value. This indicates that the mesh quality has great influence on the response of structure.

6. Conclusions

The non-linear dynamic finite element analysis software LS-DYNA is employed to investigate the damage mechanism and dynamic responses of the RC containment subjected internal blast loading. A comparison between the fine mesh and coarse mesh for the stress, pressure and displacement shows that increasing mesh quantity may improve the accuracy of the analysis results for a scale distance of $0.368\text{--}2.181 \text{ m/kg}^{1/3}$, thus, to guarantee that the results are closer to the actual situation the finite mesh division should be as fine as possible. A fluid–structure coupling algorithm and multi-material model are adopted in this study. For the 20 m standoff distance between the explosive and containment, the relative difference in the pressure and von mises stress are compared. The weakest position and failure occurred of the containment is dome which more close to the explosion source may be subjected to the strongest impact. The blast pressure wave when the explosion in the RC containment was different from free-field blast pressure due to multiple reflections during the propagation process of blast wave which was not occurred in the free filed detonation.

Acknowledgements

This study was financially supported by the Specialized Research Fund for Doctoral Program of Higher Education Institutions, China (Grant No. 20110041110012) and the State Key Program of National Natural Science of China (Grant No. 51138001).

References

- [1] R.L. Frano, G. Forasassi, Preliminary evaluation of air craft impact on a near term unclear power plant, *Nuclear Engineering and Design*. 241 (2011) 5245–5250.
- [2] B. Rebor, T. Zimmerman, Dynamic rupture analysis of reinforced concrete shells, *Nuclear Engineering and Design*. 37 (1976) 269–297.
- [3] Y. Crutzen, J. Reynue, E. Vellafane, Impulsive loading on concrete structures, SMIRT 6, Paper J, 10/11, Paris, 1981.
- [4] M. Cervera et al., Non-linear transient dynamic analysis of three dimensional structures, in: E. Hinton (Ed.), *Numerical Methods and Software for Dynamic Analysis of Plates and Shells*, Pineridge Press, Swansea, UK, 1987, pp. 320–504.
- [5] H. Abbas, Dynamic response of structures subjected to missile impact, Ph. D. Thesis. University of Roorkee, India, 1992.
- [6] Q. Dong et al., Further study on strain growth in spherical containment vessels subjected to internal blast loading, *International Journal of Impact Engineering* 37 (2010) 196–206.
- [7] C.P. Lin et al., Modeling solid thermal explosion containment on reactor HNIW and HMX, *Journal of Hazardous Materials*. 176 (2010) 549–558.
- [8] Y.J. Chen et al., Dynamic responses of discrete multi-layered explosion containment vessels with the consideration of strain-hardening and strain-rate effects, *International Journal of Impact Engineering*. 37 (2010) 842–853.
- [9] A.K. Pandey, Ram Kumar, D.K. Paul, D.N. Trikha, Non-linear response of reinforced concrete containment structure under blast loading, *Nuclear Engineering and Design*. 236 (2006) 993–1002.
- [10] H.T. Hu and Y.H. Lin, Ultimate analysis of PWR prestressed concrete containment subjected to internal pressure, *International Journal of Pressure Vessels and Piping*. 83, 161–167.

- [11] Keivan Kiani et al., Response of reinforced concrete structures to macrocell corrosion of reinforcements. Part II: After propagation of microcracks via a numerical approach. *Nuclear Engineering and Design* 242, 7–18.
- [12] Bao Xiaoli, Bing Li, Residual strength of blast damaged reinforced concrete columns, *International Journal of Impact Engineering*. 37 (2010) 295–308.
- [13] H. Hao, H.K. Cheong, S. Cui, Numerical study of dynamic buckling of steel columns subjected to underground explosion, *Key Engineering Materials* 233–236 (2002) 211–216.
- [14] R.L. Sheng, E.C. John, B.M. Kenneth, Design of reinforced concrete columns to resist the effects of suitcase bombs, in: *The 6th Asia–Pacific Conference Shock and Impact loads on Structures*, Perth W Australia, 2005, pp. 325–331.
- [15] P.T. Nash, C.V.G. Vallabhan, T.C. Knight, Spall damage to concrete walls from close-in cased and uncased explosions in air, *ACI Structural Journal* 92 (6) (1995) 680–688.
- [16] R.K. Varma, C.P.S. Tomar, S. Parkash, Damage to brick masonry panel walls under high explosive detonation, *Pressure Vessels and Piping Division PVP*, vol. 351, ASME, 1997, pp. 207–216.
- [17] D. Makovicka, Dynamic response of thin masonry wall under explosion effect, *Structures and Materials* 11 (2002) 47–56.
- [18] G.C. Mays, J.G. Hetherington, T.A. Rose, Response to blast loading of concrete wall panels with openings, *Journal of Structural Engineering* 125 (12) (1999) 1448–1450.
- [19] Y.S. Tai, Dynamic response of a reinforced concrete slab subjected to air blast load, *Theoretical and Applied Fracture Mechanics* (2011) 1–8.
- [20] W.E. Baker, *Explosions in Air*, University of Texas Press, Austin, TX, 1973, pp. 7–15.
- [21] J. Henrych, *The Dynamics of Explosion and its Use*, Elsevier Scientific Publishing Company, 1979.
- [22] H.L. Brode, Numerical solution of spherical blast waves, *Journal of Applied Physics* 26 (6) (1955).
- [23] B. Hopkinson, *British Ordinance Board Minutes*, 1915.
- [24] C. Cranz, *Lehrbuch der Ballistik*, Springer-Verlag, Berlin, 1926.
- [25] sj. Pi, D.S. Cheng, H.L. Cheng, W.C. Li, C.W. Hung, Fluid-structure-interaction for a steel plate subjected to non-contact explosion, *Theoretical and Applied Fracture Mechanics* 236 (2012) 1–7.
- [26] B.M. Dobratz, *LLNL Explosive Handbook*, UCRL-52997, Lawrence Livermore National Laboratory, Livermore, CA, 1981.
- [27] *LS-DYNA Version 970 User's Manual*, Livermore Software Technology Corporation, 2003.